Hydrogen Index measurements of highly saline brines under pressures up to 15'000 psi and temperatures up to 300°F

S. A. Hertel, B. C. Anger, K. Smith, M. Appel

Shell Exploration and Production Inc., Shell Technology Center, 3333 Highway 6 South, Houston, TX 77082

ABSTRACT

The Hydrogen Index is routinely used as a calibration factor for NMR porosity measurements in hydrocarbon reservoirs. It accounts for the reduced density of hydrogen atoms in the different pore fluids present in the porous reservoir rock. In this contribution we present an experimental setup which allows one to measure Hydrogen Indices of brines and other chemicals under reservoir conditions. The experimental data for NaCl brines agrees with a recently published density model within experimental uncertainty of $\pm 0.5\%$. The model and experimental data show that the Hydrogen Index of NaCl brines can be reduced by up to 17%. Thus, failure to account for this effect may lead to unacceptable underestimations of porosity in certain hydrocarbon reservoirs.

INTRODUCTION

Nuclear Magnetic Resonance (NMR) has been utilized in research laboratories of the hydrocarbon industry almost since its discovery by Bloch (1) and Purcell (2). During the 1990s NMR logging tools for downhole porosity and permeability measurements were established as standard tools for reservoir characterization (3). One essential calibration factor for the calculation of accurate porosity values from NMR data is the Hydrogen Index (HI). It accounts for the different densities of hydrogen nuclei in dependence of the pore fluid types (4; 5). Several studies were concerned with measuring the Hydrogen Indices of gases and live crude oils under reservoir conditions (6; 7). For brines it was pointed out that the Hydrogen Index can deviate substantially from unity at high salinities at standard temperature and pressure (4). For an estimation of the impact of such deviations, consider a formation porosity of 25% fully saturated with brine having a Hydrogen Index of 0.85. If the HI was wrongly assumed to be unity, the porosity of this formation would be under estimated by 4.4 porosity units. One common approach to calculate the HI of the brines under reservoir conditions is to use brine density data from thermodynamic tables such as ref. (8). However, empirical brine density models may prove to integrate more seamlessly into reservoir evaluation workflows. In this contribution we present an apparatus and measurements to validate a recently published density model as a tool to predict the HI of brines over a wide range of temperatures, pressures and salinities (9). At the same time the measurements were used to benchmark the equipment for future experiments involving more complex fluids and oversaturated brines.

BACKGROUND

NMR logging tools are primarily sensitive to the nuclear magnetization of the hydrogen nuclei ^{1}H of the formation fluids (10). The magnetization is given by the Curie law for spin-1/2 systems

$$M = \frac{N\gamma^2\hbar^2 B_0}{4kT},$$

(1)

where γ denotes the gyro-magnetic ratio, B_0 is the magnetic field strength, k is Boltzmann's constant and T is the temperature in Kelvin. The number of spins N in the sensitive region is itself proportional to the number of hydrogen atoms per fluid molecule N_H as well as the density $\rho(p,T)$ of the investigated fluids i.e.

$$N \propto \rho(p,T)N_H,$$

(2)

where p is the pressure. For NMR porosity measurements the Hydrogen Index is a convenient factor to account for the dependence given by eq. 2 relative to pure H_2O at Standard Temperature and Pressure (STP). Therefore, the Hydrogen Index is given by

$$
\begin{aligned}
HI &= \frac{\text{Amount of hydrogen in sample}}{\text{Amount of hydrogen in pure water at STP}} \\
&= \frac{\text{moles H / cm}^3}{0.111} \\
&= \frac{\rho(p,T)N_H/M}{0.111}.
\end{aligned}
$$

(3)

Here, M denotes the molecular weight of the pore fluid under study. In practice the NMR tool is immersed in a water tank at STP ($T = 68°F, p = 14.5$ psi) before each logging run. In the water tank a reference signal is acquired. Thereafter, the NMR logging tool is lowered into the borehole, where the sensitive region of the tool extends into the porous rock of the hydrocarbon reservoir. The NMR signal amplitude is then reduced compared to the reference signal, since the rock matrix itself is NMR silent. In this case the ratio of the signal amplitude of the pore fluids to the reference signal amplitude is proportional to the porosity (10). Several calibrations have to be applied to account for the temperature and pressure difference between STP and the reservoir conditions. These differences affect the magnetization of the fluids as well as the electronic characteristics of the NMR tool (10). It can be seen from eq. 3 that with the knowledge of the density of the brine and the molality of the salts, one may calculate the Hydrogen Index. For this work, the model for brine densities of Mao and Duan (9) was chosen. The range of validity of this model for NaCl is $T = 31.7°F - 517.7°F$ and $p = 14.5$ psi $- 14,500$ psi. The brine density ρ is given by (9)

$$\rho = \frac{(1000 + mM_s)\rho_{H_2O}}{m\,v(m)},$$

(4)

where m is the molality of salts (LiCl, NaCl, KCl, MgCl$_2$, CaCl$_2$, SrCl$_2$, BaCl$_2$) and M_s is the molar mass of the chlorides. ρ_{H_2O} is the density of pure water at the particular pressure p and temperature T and is calculated from the equations of the International Association for the Properties of Water and Steam (11). The specific solution volume $v(m) = V(m)/m$ is given by

$$v(m) = \frac{V(m_r)}{m_r} + \frac{1000}{\rho_{H_2O}}\left(\frac{1}{m} - \frac{1}{m_r}\right) + v|z_+z_-|A_V\left[h(I_m) - h(I_{m_r})\right]$$
$$+ 2v_+v_-mRT\left[B_V(m - m_r) + v_+z_+mC_V\left(m^2 - m_r^2\right)\right], \tag{5}$$

where z_+ and z_- are the charge of the cation and anion, while v_+ and v_- are the number of cation and anion charges, respectively, and $v = v_+ + v_-$. A_V is the volumetric Debye-Hückel limiting law slope which can be found in ref. (12). Furthermore, I denotes the ionic strength $I = 0.5\sum_i m_i z_i^2$ and $h(I)$ is given by $h(I) = \log_{10}(1 + 1.2I^{0.5})/2.4$. The reference solution volume $V(m_r)$ and the second and third virial coefficient B_V and C_V are given by empirical polynomials in pressure p and temperature T. The equations and the involved coefficients for $V(m_r)$, B_V and C_V can be found in Mao and Duan (9). For the case of NaCl the model has an average deviation from the published experimental data of $\pm 0.025\%$, while the experimental data considered in ref. (9) themselves have a relative uncertainty ranging from 0.001% to 0.1%.

EXPERIMENTAL

Experiments were conducted with an Oxford Instruments GeoSpec 2 NMR spectrometer with a proton Larmor frequency of $\vartheta = 2.3$ MHz and a RF-coil of diameter $d = 53$ mm. Other NMR parameters were the duration of the 90° RF-pulses of $p_{90} = 14.25\ \mu s$, the recycle delay of $t_{RD} = 20$ s and the number of scans of $NS = 128$. The maximum signal amplitude was obtained by using the magnitude of the first data point of the Free Induction Decays (FIDs). Furthermore, the dead time before detection started was increased to 100 μs to exclude spurious ^{19}F signals from the heating vessel.

A sketch of the custom built heating vessel is shown in Figure 1. From the top, one may see the high pressure tubing $(OD = 1/8'')$ that delivered pressures up to $p_{max} = 12'000$ psi provided by a Quizix QX pump (Chandler Engineering Inc). The tubing was connected to a ceramic pressure vessel (Daedalus Innovations, LLC). The ceramic pressure vessel was immersed in Fluorinert FC-70 inside a PEEK container. The FC-70 was heated to temperatures of $T_{max} = 300°F$ in a closed loop by means of a recirculation pump (Core Laboratories Inc). During the experiments at $T = 68°F$ the recirculation pump was replaced by a thermostat in order to cool the FC-70 and to achieve a smaller temperature variation compared to the recirculating pump. In order to prevent the NMR magnet from heating beyond its preset value of 95°F, a cooling loop made of Teflon tubing was wound around the outside of the PEEK vessel and cold Fluorinert FC-72 was pumped continuously through the cooling loop. In addition, cold air was blown through the spectrometer bore to dissipate any remaining heat from the PEEK container. The

assembly was lowered into the NMR spectrometer using a translation stage. The temperature of the FC-70 was continuously recorded by a thermocouple at the bottom of the PEEK vessel and a variation of $\pm2°F$ was observed over the entire duration of each experiment. However, a temperature gradient may have established between the FC-70 and the inside of the ceramic pressure vessel especially at elevated temperatures. A temperature difference of $\pm10°F$ would contribute a relative uncertainty in the HI values of $\pm2\%$ due to the polarization correction with the factor T_{exp}/T_{ref} (Curie law eq. 1).
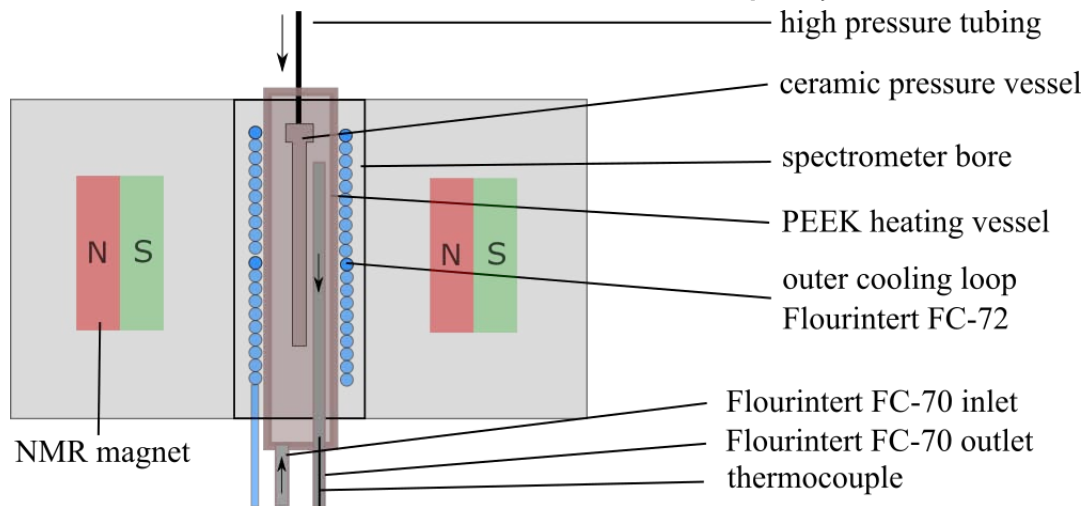
Figure 1: Sketch of the PEEK heating vessel inside the NMR spectrometer.

Six different brines were prepared with salinities of $c_s = (47, 90, 130, 170, 200, 230, 260)$ kppm. All brines were prepared by mixing pre-calculated weight fractions of NaCl salt and pure H_2O. The salinity has been double checked using a pycnometer and comparing the measured brine densities with corresponding salinity values (8).

RESULTS

The NMR reference signal was measured with degassed tap water at STP. Note that de-ionized water exhibited a too long relaxation time T_1 making the required experimental time forbiddingly long. Figure 2 shows the predicted versus measured Hydrogen Indices for pure water and the six brines with increasing salinities. The solid line is given by evaluating eq. 9, while the dashed line is given by published values (4). The experimental data and the predicted values agree within the experimental uncertainty of ±0.5 %. The primary source of uncertainty for these measurements is the signal-to-noise ratio of the NMR time domain data. It can be seen that with increasing salinity the HI of NaCl brines is reduced by up to 11%, consistent with published values (4). There is a difference of no more than 0.5% between the density model (solid line) and the published data from ref. (4) (dashed line) at salinities around 100 kppm. The reason for this difference is currently unknown since the equations used to calculate the results of ref. (4) were not explicitly stated.
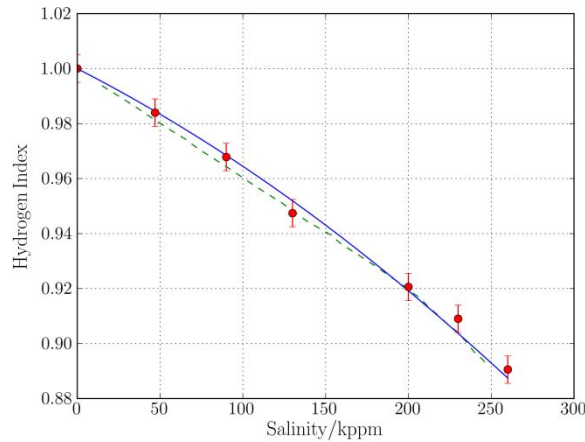
Figure 2: Plot of the Hydrogen Index versus salinity. Comparison of measured data (dots) with values predicted by the brine density model (solid line) and values taken from Kleinberg and Vinegar (4) (dashed line).

Figure 3a shows the Hydrogen Index as a function of temperature T for pure H_2O and for saturated brine with salinity of $c_s = 260$ kppm, while the pressure was fixed at $p = 5000$ psi to prevent the fluids form boiling.
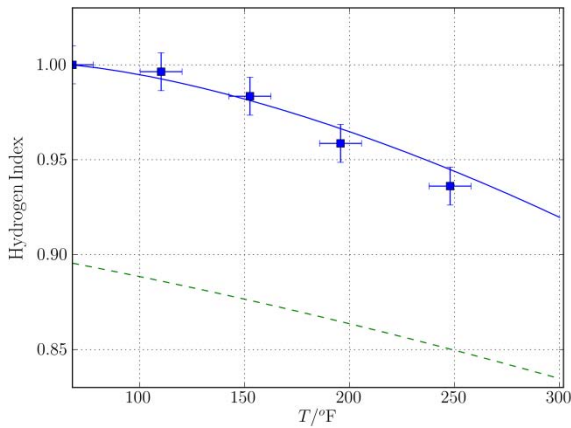
Figure 3a: Hydrogen Index versus temperature T at $p = 5000$ psi. Calculated values of HI for pure H_2O (solid line) are compared to HI for brine with salinity of $c_s = 260$ kppm (dashed line). Measured values for tap H_2O (squares).
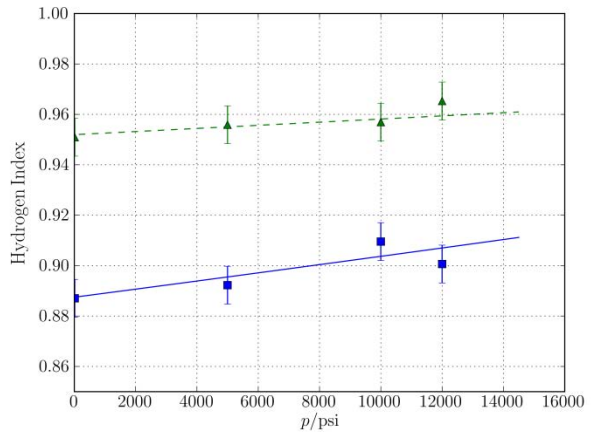
Figure 3b: Hydrogen Index versus pressure at $T = 68°F$. Calculated values for brine with salinity of $c_s = 260$ kppm (solid line) and measured values (squares) are compared to a brine with salinity of $c_s = 130$ kppm (dashed line) and corresponding measured values (triangles).

The measured signal was corrected by the ratio T_{exp}/T_{ref} to account for the difference in polarization due to the Curie law given by eq. 1. The experimental data agrees with the calculated values within the relative uncertainty of $\pm 2\%$. The higher uncertainty is a result of the higher variation of temperature T when using the recirculating pump as compared to the thermostat and the corresponding correction using the Curie law (eq. 1). The curve of H_2O (solid line) and saturated brine (dashed line) are offset due to the

salinity effect. It is interesting to note that the HI for saturated brine is reduced to $HI = 0.83$ at $T = 300°F$, a 17% decrease as compared to H_2O at STP.

Figure 3b shows the HI as a function of pressure for two brines of salinities $c_s = 260$ kppm (solid line) and $c_s = 130$ kppm (dashed line) at a temperature of $T = 68°F$. It can be seen that the effect of pressure on the HI is an increase of a moderate 2% over the entire pressure range of $p = 14.5$ psi to $p = 14,500$ psi, which is a result of the increased fluid density. A similar change of about 2% can be observed for temperatures above $T = 68°F$ (not shown). Thus, temperature and salinity of the investigated brines are the dominating effects that have to be accounted for when considering a Hydrogen Index calibration of NMR logging data.

CONCLUSION

It was shown that the experimental setup presented in this contribution can reliably measure the Hydrogen Index of brines over a wide range of pressures and temperatures. Additionally, the brine density model may be utilized to predict the HI for NaCl brines and thus can be implemented in reservoir evaluation workflows. It remains to be evaluated whether the model can be utilized to calculate the HI of brines involving mixtures of LiCl, KCl, $MgCl_2$, $CaCl_2$, $SrCl_2$ and $BaCl_2$. However, it may be necessary to experimentally determine the HI of more complex fluids and chemicals for which the setup has been shown to deliver sufficiently accurate results.

ACKNOWLEDGEMENTS

REFERENCES

1. Bloch, F., Hansen, F. F., and Packard, M., *Physical Review* (1946), **70**, 474.
2. E. M., Torrey, H. C., and Pound, R. V. *Physical Review*, (1946), 37-38.
3. Kleinberg, R. L., Jackson, J. A., Brown, R. J. S., Chandler, R., Miller, M. N., Paltiel, Z., Prammer, M. G., *Concepts in Magnetic Resonance*, (2001), **13**, 340-411.
4. Kleinberg, R. L. and Vinegar H. J., *The Log Analyst*, (1996), 20-32.
5. Appel, M., *SPWLA Petrophysics*, (2004), **45**, 296-307
6. Zhang, Q., Lo, S. L., Huang, C. C., Hirasaki, G. J., Kobayashi, R., and House,W. V. *39th Annual Logging Symposium: SPWLA*, (1998)
7. Appel, M., van Dijk, N.P., Freeman, J.J, Perkins, R.B. Dallas, *SPWLA Annual Conference and Exhibition* (2000)
8. Weast, R.C., [ed.]. *CRC Handbook of Chemistry and Physics*, Boca Raton, Florida: CRC Press, (1982), D232-D233.
9. Mao, S., Duan, Z., *The Journal of Chemical Thermodynamics*, (2008) **40**, 1046–1063
10. Coates, G. R., Xiao, L., Prammer, M. G. *Halliburton Energy Services*, (1999)
11. Wagner, W., Cooper, J. R., *J. Eng. Gas Turbines & Power*, (2000) **122**, 150-182.
12. Bradley, D.J., Pitzer, K.S., *J. Phys. Chem.*, (1979), 1599-1603